Magnetic and Thermodynamic Properties of the Three-Dimensional Periodic Anderson Hamiltonian

Carey Huscroft,[1] A. K. McMahan,[2] and R. T. Scalettar[1]
[1]*Physics Department, University of California, Davis, California 95616*
[2]*Lawrence Livermore National Laboratory, University of California, Livermore, California 94550*
(Received 8 September 1998)

The three-dimensional periodic Anderson model is studied with the quantum Monte Carlo method. We find that the crossover to the Kondo singlet regime is remarkably sharp at low temperatures, and that the behavior of magnetic correlations is consistently reflected in both the thermodynamics and the density of states. The abruptness of the transition suggests that energy changes associated with the screening of local moments by conduction electrons might be sufficient to drive large volume changes in systems where applied pressure tunes the ratio of interband hybridization to correlation energy. [S0031-9007(99)08711-6]

PACS numbers: 71.10.Fd, 71.27.+a

The problem of localized, highly correlated electrons hybridizing with a conduction band is one of long-standing interest [1]. Our understanding of the underlying physics has recently been increased through new analytic approaches [1,2], and numeric methods like quantum Monte Carlo (QMC) [3,4]. These techniques have emphasized the connection between static magnetic properties and the dynamic response like the density of states.

However, what has been much less carefully explored by QMC is the link to thermodynamics. An intriguing problem for which a detailed understanding of the thermodynamics is essential is the "volume-collapse" transition in rare-earth metals. This phenomenon occurs with the application of pressure to certain Lanthanides and gives rise to first order phase transitions with unusually large volume changes (14% for cerium and 9% for praseodymium) [5,6]. Accompanying the change in volume is a change in the magnetism: On the expanded, highly correlated side of the transition, the f electrons have well-defined moments, while on the contracted, less correlated side these moments disappear or are expected to disappear. The low-volume α phase of Ce is paramagnetic, as are the early actinides which are considered to be analogs for the collapsed rare-earth phases [6].

Even the qualitative origin of this phenomenon is still under debate. One suggestion is that the pressure-induced change in the ratio of the interaction strength to bandwidth gives rise to a Mott transition of the $4f$ electrons accompanied by loss of magnetic order [7]. An alternate proposition is that the rapid change in the $4f$ valence electron coupling leads to a "Kondo volume collapse" [8]. In both cases, there are dramatic thermodynamic (e.g., pressure-volume) as well as magnetic signatures of the phenomenon.

In this paper we will establish the connection between the thermodynamics and the magnetic properties of the symmetric periodic Anderson model (PAM) in three dimensions. While previous efforts have focused on the Anderson impurity model [8,9], the capabilities of modern massively parallel computers now make feasible rigorous QMC calculations for the more realistic periodic model, which has so far received little attention in three dimensions. Our key results are as follows:

(i) The dependence of the singlet correlation function on the interband hybridization shows an increasingly sharp structure as the temperature is lowered, indicating a very rapid crossover between a regime where the f sites have unscreened moments and one in which the moments are quenched by the conduction electrons.

(ii) A sharp thermodynamic feature exists at the same interband hybridization as this change in the singlet correlator. To analyze this, we introduce a new approach to the calculation of the free energy F, and show it obeys various analytic sum rules.

(iii) The pressure difference at the transition inferred from F is reasonably consistent with experimental pressure-volume data on Ce, Pr, and Gd, given the approximate representation of the electronic structure.

The periodic Anderson Hamiltonian is

$$H = \sum_{k\sigma} \epsilon_k d^\dagger_{k\sigma} d_{k\sigma} + \sum_{k\sigma} V_k (d^\dagger_{k\sigma} f_{k\sigma} + f^\dagger_{k\sigma} d_{k\sigma}) + U_f \sum_i \left(n_{if\uparrow} - \frac{1}{2}\right)\left(n_{if\downarrow} - \frac{1}{2}\right) + \sum_{i\sigma} \epsilon_f n_{if\sigma} - \mu \sum_{i\sigma} (n_{if\sigma} + n_{id\sigma}). \quad (1)$$

We choose a simple cubic structure for which

$$\epsilon_k = -2t_{dd}[\cos k_x a + \cos k_y a + \cos k_z a], \qquad V_k = -2t_{fd}[\cos k_x a + \cos k_y a + \cos k_z a], \quad (2)$$

where a is the lattice constant. The dispersion of V_k reflects our choice of near-neighbor (as opposed to on-site) hybridization of the f and d electrons. With on-site hybridization, the PAM in the Hartree-Fock approximation

 0031-9007/99/82(11)/2342(4)$15.00

is an insulator at the half-filled symmetric point and a metal at slightly different filling, whereas our intersite hybridization choice is always a metal in this approximation, making it a more plausible starting point for describing the metallic rare earths. Parameter values and temperature T in this work are given in units of t_{dd}. We take $U_f = 6$, consistent with the rare earths for a reasonable choice of $t_{dd} = 1$ eV, and explore a range of t_{fd} and T values. QMC results for this model were obtained using the determinant algorithm [10], which provides an exact treatment (to within statistical errors and finite size effects) of the correlations. We further choose the symmetric PAM ($\mu = \epsilon_f = 0$, and thus half-filling: $\langle n_{if}\rangle = \langle n_{id}\rangle = 1$) in order to eliminate the QMC "sign problem," allowing accurate simulations at lower temperatures.

Figure 1 shows the temperature and t_{fd} dependence of the singlet correlation function summed over near neighbors of a given site **i**,

$$c_{fd} = \sum_{\mathbf{j}}^{nn} \langle \vec{S}_{f\mathbf{i}} \cdot \vec{S}_{d\mathbf{j}} \rangle . \tag{3}$$

Here $\vec{S}_{f\mathbf{i}} = (f^\dagger_{\uparrow\mathbf{i}}\ f^\dagger_{\downarrow\mathbf{i}})\vec{\sigma}\binom{f_{\uparrow\mathbf{i}}}{f_{\downarrow\mathbf{i}}}$ and similarly for $\vec{S}_{d\mathbf{j}}$. For weak hybridization t_{fd} the f moments are unscreened by the conduction electrons and c_{fd} is small. At low temperature, a sharp change is seen to occur at $t_{fd} \approx 0.6$ to a phase where such screening is well established.

This sharp switch is also reflected in the energy E and free energy F. The difference $\Delta E(T) = E_{\mathrm{QMC}}(T) - E_{\mathrm{AFHF}}(T)$ of the QMC calculations relative to antiferromagnetic Hartree-Fock (AFHF) results at the same temperature ($T = 0.08$) is shown in Fig. 2(a). To get $F = E - ST$ we fit [11] the raw data for $E_{\mathrm{QMC}}(T)$,

$$E_{\mathrm{QMC}}(T) = E_0 + \sum_n c_n e^{-n\Delta/T}. \tag{4}$$

The number of fitting parameters (E_0, c_n, Δ) was taken to be about half of the number of data points. The entropy is then [12],

$$S(T) = S_0 + \frac{1}{T}\sum_n c_n \left(1 + \frac{T}{n\Delta}\right) e^{-n\Delta/T}. \tag{5}$$

Figure 3 shows a plot of the resulting free energy difference $\Delta F(T) = F_{\mathrm{QMC}}(T) - F_{\mathrm{AFHF}}(T)$. Independent fits (E_0, c_n, Δ) were performed for each t_{fd}, so that the smoothness of the resultant curves in Fig. 3 is one measure of the success of this procedure. Another is that our fit yields $\sum_n c_n/n\Delta$ to within ~3% of the expected value [12] for $t_{fd} \geq 0.8$. This sum is smaller by $\ln 2$ to within ~3% for $t_{fd} \leq 0.5$, reflecting magnetic disorder of the spins below our lowest temperature ($T = 0.08$) in this regime, and consequent validity of the fit only for $T \geq 0.08$.

The crucial feature in Figs. 2(a) and 3 is the rapid change in slope at low temperatures of ΔE and ΔF near $t_{fd} = 0.6$. This behavior is hard to discern in the full thermodynamic functions whose variation with t_{fd} is ~20 times larger than seen for these difference functions. It arises from the QMC results as the HF solution is smooth and without phase transitions throughout the t_{fd}, T region plotted here. Moreover, HF provides the natural reference for this subtraction as it gives the exact ground state at $t_{fd} = 0$ and its free energy is an upper bound on the exact QMC result at all T and t_{fd}. The size of the present slope

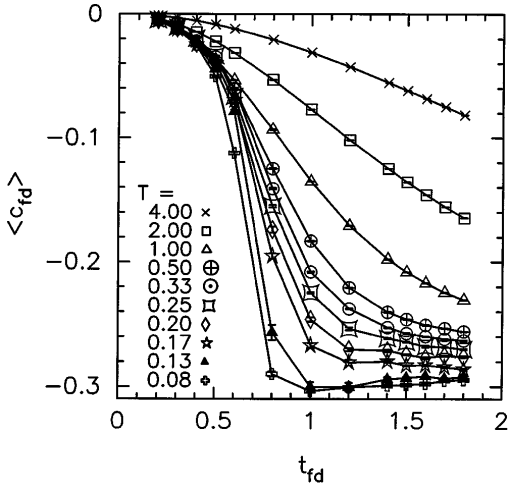

FIG. 1. The singlet correlation function c_{fd} as a function of f-d hybridization. As the temperature is lowered, there is an increasingly rapid switch from a small t_{fd} regime where singlet correlations are absent to a large t_{fd} regime where Kondo singlets are well formed. Error bars are visible when larger than symbol size.

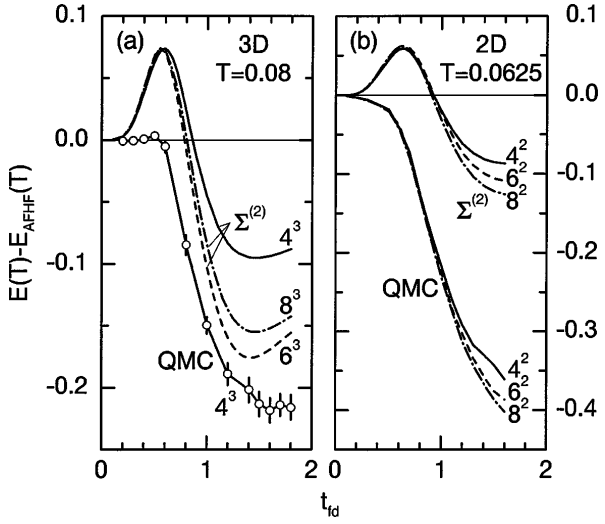

FIG. 2. (a) The difference in energies between QMC and antiferromagnetic Hartree-Fock solutions. At small t_{fd}, the AFHF energy accurately tracks the QMC. However, at intermediate coupling the QMC results break away, reflecting the failure of HF to pick up the singlet correlations. (b) 2D QMC data allow an assessment of finite size effects, along with a perturbation approach [14], labeled $\Sigma^{(2)}$, shown for both 2D and 3D. 3D QMC error bars are shown where larger than the symbol size; 2D QMC error bars are ≤ 0.01 in size.

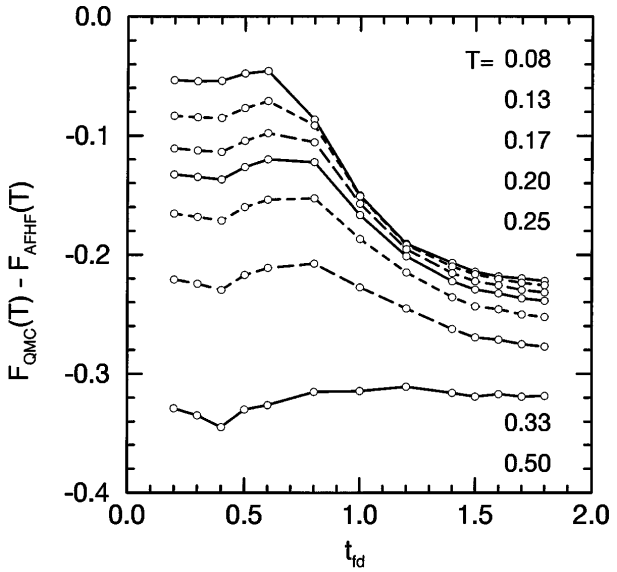

FIG. 3. The difference in free energies between QMC and antiferromagnetic Hartree-Fock solutions. At strong coupling (small t_{fd}) the agreement in the free energy is good apart from an overall shift of $T \ln 2$ associated with the tendency of HF to overestimate the magnetic order. As in Fig. 2(a), at intermediate coupling ΔF becomes sizable.

change is not inconsistent with the volume collapse transitions, where one might view $\Delta F = \min(F_1, F_2) - F_1$ with F_1 and F_2 being free energy branches associated with the small t_{fd} (large volume) and large t_{fd} (small volume) phases, respectively. Given a volume dependence [6] of $t_{fd} \sim V^{-2}$, the slope change is related to a pressure difference by $V\Delta P/2 = -(1/2)\partial\Delta F/\partial \ln V \sim \partial\Delta F/\partial \ln t_{fd}$. Extrapolations of experimental pressure-volume data [13] into the two phase regions suggests $V\Delta P/2 \sim 0.4$, 0.5, and 1.3 eV for Ce, Pr, and Gd, respectively. The low-T slope change in Figs. 2(a) and 3 is $\partial\Delta F/\partial \ln t_{fd} =$ 0.2–0.3 eV, which given the crudeness of the present representation of the rare-earth valence electrons is reasonably consistent.

The QMC calculations were carried out for a 4^3-site periodic lattice. As a systematic exploration of system size for these three-dimensional (3D) calculations would be prohibitive, we have used 2D QMC calculations, Fig. 2(b), as well as a second-order self-energy approach [14], labeled $\Sigma^{(2)}$ in Fig. 2, to estimate the size effects. While offset from the QMC results, the 2D $E_{\Sigma^{(2)}} - E_{\mathrm{AFHF}}$ curves in Fig. 2(b) for 4^2, 6^2, and 8^2-site lattices reasonably approximate the finite size effects in the 2D QMC. We expect the $\Sigma^{(2)}$ calculations in Fig. 2(a) to provide a comparable indication in 3D, suggesting that finite size effects do not alter the qualitative physics [15], and if anything, may serve to increase $\partial\Delta F/\partial \ln t_{fd}$, improving agreement with experiment.

There is striking consistency between the singlet correlations in Fig. 1 and the energy and free energy differences in Figs. 2(a) and 3. In all cases there is a rather abrupt switch in low-T behavior across $t_{fd} \sim 0.6$, which anneals with increasing temperature. The anomalies are largely gone above $T \sim 0.5$, an upper bound for what might be a critical temperature in the present model. The actual critical temperature will reflect competition between effects like these in ΔF and the volume dependence of a realistic generalization of F_{AFHF}. An important term in ΔF is the QMC entropy, which reflects disordered spins for small t_{fd} at the lowest temperature $T = 0.08$, in contrast to larger t_{fd} values at this temperature, as well as the stable AFHF solution throughout the range plotted in Fig. 3, where the entropy is approximately minimal. Consequently, ΔF includes a $-T \ln 2$ entropy term at small t_{fd}, but not at large t_{fd}, which serves to level out the ΔF curves as temperature is increased.

Besides singlet formation, magnetic ordering of the local moments is a generic feature of the PAM. Indeed, our calculations of the f-f structure factor suggest a strong tendency for the f moments to order antiferromagnetically at low temperatures with a maximal ordering temperature in the vicinity of $t_{fd} = 0.8$. Further insight into the relation between AF, singlet formation, and the thermodynamics can be obtained by computing the heat capacity $C(T) = dE(T)/dT$ [6]. We find a low-temperature peak similar to recent work on the two-dimensional Hubbard model [11], with an area $\int dTC(T)/T$ of $\ln 2$ at small t_{fd}, which, however, washes out with decreasing area at large t_{fd}. The peak has only minor impact on the slope change discussed above for ΔE_{QMC} and ΔF_{QMC} as functions of t_{fd} [16].

A more complete picture of the PAM is given by the density of states, $N_f(\omega)$, which we obtain using the maximum entropy method [17] to perform the analytic continuation of the imaginary time Greens function computed in QMC. The results for different t_{fd} at fixed $T = 0.2$ are shown in Fig. 4. $N_f(\omega)$ evolves from a structure with upper and lower Hubbard bands separated by a gap U_f at small t_{fd} to a regime where broadened remnants of these bands are still evident, but additional resonant peaks characteristic of Kondo singlet formation have also developed. These first appear with increasing t_{fd} at $t_{fd} \approx$ 0.6. Further increase in t_{fd} enhances the weight in this central region at the expense of the Hubbard sidebands.

The precise nature of the gap in the density of states at the Fermi surface, $\omega = 0$, is still open to interpretation. For the half-filled, single band Hubbard Hamiltonian, $N(\omega)$ has a similar gap which evolves continuously from predominantly Mott-Hubbard character, for $U \gg W$, to a Slater gap associated with antiferromagnetic order, for $U \ll W$. Similarly, the two-band model considered here has a Mott gap at small t_{fd}, while the gap at larger t_{fd} could originate either as a result of long range antiferromagnetic order on the f sites, or, alternately, reflect a "coherence gap" associated with singlet formation. The competition between these two latter effects on $N(\omega)$ is well documented in a lower dimension

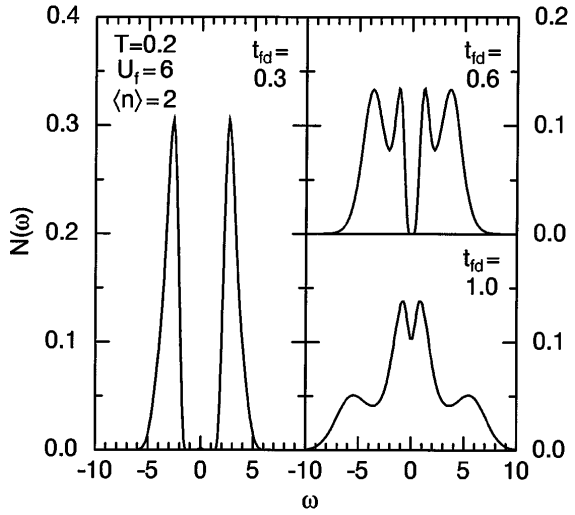

FIG. 4. The f-band density of states for different f-d hybridization. For weak hybridization, there are peaks at $\pm U_f/2$. These broaden with increasing t_{fd}, and a Kondo resonance develops.

[4]. Here, studies of the f-f correlation function show no signs of antiferromagnetic long-range order (AFLRO) at $t_{fd} = 0.6$ and $T = 0.2 > T_{\mathrm{Neel}}$, which suggests these resonances signal singlet formation, not AFLRO. Analytic continuation of two particle Green's functions, like the magnetic susceptibility, will lend further insight into this question.

In this paper we have shown that there is a striking consistency between the location of sharp crossovers in the singlet magnetic and thermodynamic properties of the three-dimensional periodic Anderson model. The f density of states shows a structure expected to arise from singlet correlations. Finally, estimates of the associated change in free energy are of the same order of magnitude as observed in the rare-earth volume collapse transitions.

Two important issues remain open. The first is the extension to Hamiltonians with the full rare-earth orbital complexity. Initial studies of how the Mott transition varies with band degeneracy in the Hubbard model, and other issues, already exist [18] within approximate numerical approaches like dynamical mean-field theory [2]. The second, related, issue concerns band filling. Studies with many f orbitals will require working away from the symmetric point.

Work at UCD was supported in part by an Accelerated Strategic Computing Initiative grant and by the LLNL Materials Institute; that at LLNL, by the U.S. Department of Energy under Contract No. W-7405-Eng–48. The QMC calculations were performed on the ASCI Blue-Pacific and Red platforms.

[1] G. R. Stewart, Rev. Mod. Phys. **56**, 755 (1984); P. A. Lee *et al.*, Comments Condens. Matter. Phys. **12**, 99 (1986); A. C. Hewson, *The Kondo Problem to Heavy Fermions* (Cambridge University Press, Cambridge, 1993).

[2] D. Vollhardt, in *Correlated Electron Systems*, edited by V. J. Emery (World Scientific, Singapore, 1993), p. 57; A. Georges *et al.*, Rev. Mod. Phys. **68**, 13 (1996); Th. Pruschke *et al.*, Adv. Phys. **44**, 187 (1995).

[3] J. Bonča and J. E. Gubernatis, Phys. Rev. B **58**, 6992 (1998); Y. Zhang and J. Callaway, Phys. Rev. B **38**, 641 (1988); M. Jarrell, Phys. Rev. B **51**, 7429 (1995); A. N. Tahvildar-Zadeh *et al.*, Phys. Rev. B **55**, 3332 (1997); M. Rozenberg, Phys. Rev. B **52**, 7369 (1995).

[4] M. Vekic *et al.*, Phys. Rev. Lett. **74**, 2367 (1995).

[5] See, e.g., U. Benedict *et al.*, Physica (Amsterdam) **144B**, 14 (1986).

[6] A. McMahan *et al.*, J. Comput.-Aided Mater. Des. **5**, 131 (1998).

[7] B. Johansson, Philos. Mag. **30**, 469 (1974).

[8] J. W. Allen and R. M. Martin, Phys. Rev. Lett. **49**, 1106 (1982); J. W. Allen and L. Z. Liu, Phys. Rev. B **46**, 5047 (1992); M. Lavagna *et al.*, Phys. Lett. **90A**, 210 (1982); J. Phys. F **13**, 1007 (1983).

[9] O. Gunnarsson and K. Schonhammer, Phys. Rev. B **28**, 4315 (1983).

[10] R. Blankenbecler *et al.*, Phys. Rev. D **24**, 2278 (1981).

[11] For an alternate method, see D. Duffy and A. Moreo, Phys. Rev. B **55**, 12 918 (1997).

[12] The constant $S_0 \equiv 4 \ln 2 - \sum_n c_n/n\Delta$, and should equal $(2N_0/N) \ln 2$ where N_0 is the number of discrete k points which have $\epsilon_k = V_k = 0$ on a finite lattice. $N_0/N \to 0$ as $N \to \infty$.

[13] See Ref. [6], Fig. 1 and references therein.

[14] M. M. Steiner *et al.*, Phys. Rev. B **43**, 1637 (1991); H. Schweitzer and G. Czycholl, Solid State Commun. **74**, 735 (1990).

[15] Local quantities like the energy and singlet correlations show relatively smaller finite size effects.

[16] One way to see this is from Fig. 2(a). The paramagnetic $\Sigma^{(2)}$ calculation in Fig. 2 has no low-T peak in $C(T)$, yet yields structure similar to the full QMC results. Moreover, with guidance from the temperature dependence of $E_{\Sigma^{(2)}}(T)$, one may extrapolate low-T "QMC" energies for which the $C(T)$ peak has been artificially removed. These modified QMC energies yield a ΔE_{QMC} curve only slightly different from that in Fig. 2(a).

[17] M. Jarrell and J. E. Gubernatis, Phys. Rep. **269**, 135 (1996).

[18] M. H. Hettler *et al.*, Phys. Rev. B **58**, 7475 (1998); H. Kajueter and G. Kotliar, Int. J. Mod. Phys. B **11**, 729 (1997); O. Gunnarsson *et al.*, Phys. Rev. B **56**, 1146 (1997); J. Bunemann *et al.*, Phys. Rev. B **57**, 6896 (1998); Y. Motome and M. Imada, J. Phys. Soc. Jpn. **66**, 1872 (1997).